Wednesday, September 17, 2008

The atmospheric impact of the Carrington event solar protons

Craig J. Rodger

Department of Physics, University of Otago, Dunedin, New Zealand

Pekka T. Verronen

Finnish Meteorological Institute, Helsinki, Finland

Mark A. Clilverd and Annika Seppälä

Physical Sciences Division, British Antarctic Survey (NERC), Cambridge, United Kingdom

Esa Turunen

Sodankylä Geophysical Observatory, University of Oulu, Sodankylä, Finland

Abstract. The Carrington event of August/September 1859 was the most significant solar proton event (SPE) of the last 450 years, about four times larger than the solar proton fluence of the largest event from the "spacecraft era" (August 1972). Recently, much attention has focused upon increasing our understanding of the Carrington event, in order to better quantify the impact of extreme space weather events. In this study the Sodankylä Ion and Neutral Chemistry (SIC) model is used to estimate the impact of the Carrington event to the neutral atmosphere and the ionosphere, and the disruption to HF communication. We adopt a reported intensity-time profile for the solar proton flux, and examine the relative atmospheric response to different SPE-energy spectra, and in particular, the comparatively soft energy spectrum of the August 1972 or March 1991 SPE which are believed to provide the best representation of the Carrington event. Our calculations indicate that large changes in electron density and atmospheric constituents occur during the period of SPE-forcing, depending upon the nature of the spectrum and also on the hemisphere considered. However, the most important SPE-driven

atmospheric response is an unusually strong and long-lived O_x decrease in the upper stratosphere (O_x levels drop by ~40%) primarily caused by the very large fluxes of >30 MeV protons. This depletion is an indication of the extreme changes possible for the largest SPE. We find that there are comparatively small long-term differences in the atmospheric and ionospheric response between the 3 suggested SPE spectra.

1. Introduction

The Carrington event of August/September 1859 was the most significant solar proton event (SPE) of the last 450 years, identified through impulsive nitrate events in polar ice [*McCracken et al.*, 2001]. The >30 MeV solar proton fluence determined from the ice cores indicate it was twice as large as the next largest event (1895), and roughly four times larger than the solar proton fluence of the largest event from the "spacecraft era" which occurred in August 1972. The Carrington SPE was associated with the 1–2 September 1859 magnetic storm, the most intense in recorded history [*Tsurutani et al.*, 2003]. The space weather events of August/September 1859 are now particularly famous due to Carrington's visual observation of a white-light solar flare for the first time [*Carrington*, 1960]. The associated magnetic disturbances produced widespread auroral displays and disruption to telegraph transmissions which attracted much public attention and were widely reported in the newspapers and scientific articles [see the review *Boteler*, 2006].

Recently, much attention has focused upon increasing our understanding of the Carrington event, in order to better quantify what extreme space weather events could do to our current technological society. For example, estimates suggest a potential economic loss of <US$70 billion due to lost revenue (~US$44 billion) and the cost of replacement of GEO satellites (~US$24 billion) caused by a "once a century" single storm similar to the Carrington event

[*Odenwald et al.*, 2006]. These authors estimate that 80 satellites in low-, medium, and geostationary- Earth orbits might be disabled as a consequence of a superstorm event with additional disruptions caused by the failure of many of the satellite navigation systems (e.g., GPS). Ionising radiation doses from the SPE have been estimated to be as high as 54 krad (Si) [*Townsend et al.*, 2003], levels which are not only highly life-threatening for crews of manned missions, but present a significant hazard to onboard electronics.

Solar proton events produce large ionization changes in the polar ionosphere which can drive significant changes in atmospheric chemistry and communications disruption. Over the years several studies of Solar Proton Event effects on the atmosphere have been published. The earlier work of *Crutzen and Solomon* [1980], *McPeters et al.* [1981], and *Solomon et al.* [1983] has been followed by several studies, notably the work of Jackman and coauthors [*Jackman and McPeters*, 1985; *Jackman and Meade*, 1988; *Jackman et al.*, 1990, 1993, 1995, 2000]. SPEs result in enhancements of odd nitrogen (NO_x) and odd hydrogen (HO_x) in the upper stratosphere and mesosphere [*Crutzen et al.*,1975; *Solomon et al.*, 1981; *Jackman et al.*, 1990, 2000]. NO_x and HO_x play a key role in the ozone balance of the middle atmosphere because they destroy odd oxygen through catalytic reactions [e.g., *Brasseur and Solomon,* 1986, pp. 291-299]. Ionization changes produced by a 20 MeV proton will tend to peak at ~60 km altitude [*Turunen et al.,* Fig 3, 2008]. Ionization increases occurring at similar altitudes, caused by solar proton events are known to lead to significant local perturbations in ozone levels [*Verronen et al.*, 2005], with polar ozone levels decreasing by >50% for large SPE. However, the effect on annually averaged global total ozone is considered to be relatively small, of the order of few tenths of a percent at the maximum [*Jackman et al.*, 1996]. Changes in NO_x and O_3 consistent with solar proton-driven modifications have been observed [*Jackman et al.* ,2001; *Seppälä et al.*, 2004; *Verronen et al.*, 2005]. It is well-known that particle precipitation at high latitudes produce additional ionization leading to increased HF absorption at high-latitudes

[*MacNamara*, 1985], in extreme cases producing a complete blackout of HF communications in the polar regions.

In order to consider the impact of the Carrington event solar protons upon the Earth's atmosphere, information on the fluence and energy spectrum of the SPE is required. An estimate of the odd nitrogen increases and ozone decreases due to the Carrington SPE has been undertaken [*Thomas et al.*, 2007], using a Greenland ice core derived >30 MeV fluence of 2.7×10^{10} cm^{-2} and a spectrum taken from the very energetic and spectrally hard 19 October 1989 SPE. The total ionization was distributed over the 2 day duration uniformly (i.e. as a step function), leading to a localized maximum column ozone depletion which was ~3.5 times greater than that of the 1989 event. As noted in this study, the use of the 19 October 1989 spectrum to represent the 1859 Carrington SPE was a "best guess" approach, given the total lack of direct proton spectral measurements in that era.

Limits on the Carrington event spectrum have been provided by measurements of the cosmogenic isotope ^{10}Be, also found in polar ice cores. Analysis of the ^{10}Be concentrations suggest that the spectral hardness of the Carrington event was significantly softer than those of September-October 1989 SPE [*Beer et al.*, 1990]; any increase in ^{10}Be associated with the Carrington event was found to be less than the 9% standard deviation of the annual data. It has been suggested that the Carrington event may have had an energy spectrum very similar to those measured for the August 1972 or March 1991 SPE [*Smart et al.*, 2006]. The later study also constructed an intensity-time profile of the solar particle flux, by assuming that the Carrington solar event is part of the class of interplanetary shock-dominated events where the maximum particle flux is observed as the shock passes the Earth.

In this study we make use of the new findings as to the nature of the Carrington event, adopting both the *Smart et al.* [2006] intensity-time profile for the >30 MeV solar proton flux, and the softer energy spectrum required to reproduce the cosmogenic isotope concentrations.

We make use of the Sodankylä Ion and Neutral Chemistry (SIC) model to estimate the impact of the Carrington event to the neutral atmosphere and the ionosphere, and the disruption to HF communication. We go on to consider the potential "worst case" significance of a Carrington-level "superstorm".

2. Spectrum and intensity-time profile of the Carrington SPE

As noted above, cosmogenic isotope concentrations have indicated that the Carrington SPE was significantly softer than those of September-October 1989 SPE. *Smart et al.* [2006] concluded that either of the comparatively soft SPE energy spectra from August 1972 or March 1991 could be representative of that for the Carrington event, given the cosmogenic isotope observations. In contrast, some previous studies into the potential doses to humans and electronics, and the atmospheric impact, have used hard SPE energy spectra, particularly 29 September 1989 and 19 October 1989 [see the discussion in *Townsend et al.*, 2006]. In this study we model the SPE spectra using a Weibull distribution, which has been shown to provide an accurate representation of the measured proton spectra for these events [*Xapsos et al.*, Table 1, 2000]. The Weibull distribution fit for differential SPE fluxes are described through the expression

$$\frac{d\Phi}{dE} = \Phi_0 k \alpha E^{\alpha-1} \exp\left(-kE^{\alpha}\right) \quad (1)$$

where E is the energy in MeV and Φ_0, k, and α are the Weibull fitting parameters. k and α are taken from *Xapsos et al.* [2000], while Φ_0 is scaled to reproduce the >30 MeV proton fluence for the Carrington event (1.9×10^{10} cm^{-2} [*McCracken et al.*, 2001]). These values are given in Table 1. The SPE fluxes are expressed with units of protons $cm^{-2}s^{-1}sr^{-1}MeV^{-1}$. Figure 1 shows a comparison between the differential fluences which have been used to describe the Carrington event, based on four different SPE. The differential fluences shown in Figure 1 have been normalised to the Carrington-level >30 MeV fluence of 1.9×10^{10} protons cm^{-2}. As noted by *Townsend et al.* [2006], both of the SPEs which occurred in 1989 were spectrally hard, and rather similar to one-another. In contrast, the SPEs which occurred in August 1972 and March 1991 were much softer, with the August 1972 SPE having an unusually soft spectrum. These two soft-spectra SPEs provide two possibilities through which we can estimate the impact of the Carrington event upon the neutral atmosphere, following the approach of *Smart et al.* [2006] to treat these as "indicative spectra". The harder spectra from September-October 1989 provide an approach by which comparisons can be made with earlier studies, and also an estimate of the possible "extreme" worst-case for a Carrington-level SPE with a hard spectra. As the September and October 1989 SPE have very similar spectra, we arbitrarily select October 1989. Note, however, that the differences between the normalised energy spectra for the two hard SPEs and that of March 1991 are much smaller across the energy range 2-40 MeV. Protons in this energy range deposit most of their energy in the altitude range ~50-85 km [*Turunen et al.*, Fig. 3, 2008], where SPE-induced changes to the neutral atmosphere are largest [e. g., *Verronen et al.*, 2005]. As such, it is instructive to contrast the atmospheric impact of the differing spectra, as this may be less significant than Figure 1 suggests.

The upper panel of Figure 2 shows the intensity-time profile for >30 MeV solar proton fluxes during the Carrington event [after Fig. 12, *Smart et al.*, 2006]. This profile is combined with the SPE energy spectra of Figure 1 to produce three different time-varying differential proton fluxes for proton energies of 1-2000 MeV across the time period of the Carrington event, as shown in the 3 lower panels of Figure 2. In those panels the time-varying differential proton flux is shown with units of $\log_{10}$[protons $cm^{-2}s^{-1}sr^{-1}MeV^{-1}$]. The second and third panels of Figure 2 represent differing possible differential fluxes for the Carrington SPE, while the lower panel represents the "worst case" of a Carrington-level SPE with a hard spectrum. For time periods outside the Smart et al. intensity-time profile, the proton fluxes are set to zero. A widely accepted SPE definition requires the >10 MeV proton flux to be >10 $cm^{-2}s^{-1}sr^{-1}MeV^{-1}$. The beginning and end of the time profile shown in Figure 2 are below this level, and thus we have confidence that the fluxes shown in Figure 2 describe the entire SPE event.

3. Sodankylä Ion Chemistry Model

Using the Sodankylä Ion and Neutral Chemistry (SIC) model we consider the atmospheric consequences of the Carrington SPE using the time-varying proton fluxes from Figure 2. SPE produce ionization increases in the polar mesosphere and upper stratosphere, which in turn alters atmospheric chemistry through changes in HO_x and NO_x. The SIC model is a 1-D chemical model designed for ionospheric D-region studies, solving the concentrations of 65 ions at altitudes across 20–150 km, of which 36 are positive and 29 negative, as well as 15 minor neutral species. Our study made use of SIC version 6.9.0. The model has recently been discussed by *Verronen et al.* [2005], building on original work by *Turunen et al.* [1996] with neutral species modifications described by *Verronen et al.* [2002]. A detailed overview of the model was given in *Verronen et al.* [2005], but we summarize the key characteristics of the model here to provide background for this study.

In the SIC model several hundred reactions are implemented, plus additional external forcing due to solar radiation (1–422.5 nm), electron and proton precipitation, and galactic cosmic radiation. Solar flux is calculated with the SOLAR2000 model (version 2.27, now the Solar Irradiance Platform, SIP) [*Tobiska et al.*, 2000]. The scattered component of solar Lyman-α flux is included using the empirical approximation given by *Thomas and Bowman* [1986]. The SIC code includes vertical transport [*Chabrillat et al.*, 2002] which takes into account molecular [*Banks and Kockarts*, 1973] and eddy diffusion with a fixed eddy diffusion coefficient profile which has a maximum of 1.2×10^6 cm^2s^{-1} at 110 km. The background neutral atmosphere is calculated using the MSISE-90 model [*Hedin*, 1991] and tables given by *Shimazaki* [1984]. The

SIC-models does not calculate temperature variations, leaving these fixed by MSIS. As such no transport driven by adiabatic heating or cooling are included in the SIC results. Such changes in vertical transport have been calculated for large SPE events [*Jackman et al.*, 2007], but were insignificant below 60 km altitudes. In the SIC model transport and chemistry are advanced in intervals of 5 minutes. Within each 5 minute interval exponentially increasing time steps are used because of the wide range of chemical time constants of the modeled species.

3.1 Control Run

In order to interpret the SPE-driven changes, a SIC modeling run has also been undertaken without any SPE-forcing (i.e., zero proton fluxes), termed the "control" run. The SIC model is run for the northern hemisphere location (70ºN, 0ºE) and southern hemisphere location (70ºS, 0ºE) starting on 27 August 1859 and continuing for 24 days. These locations were selected as the geomagnetic cutoff energy is small for sufficiently high magnetic latitudes, such that the proton flux spectra is essentially unaffected by the geomagnetic field, particularly for the mesospheric altitudes of interest. Modeling of the 1850 geomagnetic field suggests there is little change in cutoff rigidities for these locations relative to the modern field [*Shea and Smart*, Fig. 4, 2006], and hence modern rigidity calculations can be applied [e.g., *Rodger et al.*, 2006a]. In addition, for these locations UT=LT, making interpretation easier. Finally, the northern location is the same as has been used in some previous SIC-modeling studies into SPE-effects [e.g., *Verronen* et al., 2005; *Clilverd et al*, 2006; *Seppälä et al.*, 2006], allowing direct comparisons.

We assume active solar cycle phase for the SOLAR2000 output (F10.7 = 158.2×10^{-22} $Wm^{-2}Hz^{-1}$, F10.7A = 167.7×10^{-22} $Wm^{-2}Hz^{-1}$), and drive the MSIS model with Ap = 138 based on the mean storm value determined for the Carrington period [*Nevanlinna*, 2006]. Note that the geomagnetic amplitude index C9 from the St. Petersburg observatory (Russia) reached peak values of 8 and 9 for the times of the two peaks in the SPE fluxes [*Nevanlinna*, Fig 3., 2006], which will also ensure that the cutoff rigidities are very low for our modeling locations. We therefore assume that the geomagnetic cutoff energy is zero throughout the calculation for both locations.

The results of this no-forcing control SIC-run, shown in Figure 3, represent the calculation of "normal" conditions, and hence allow an indication of the significance of the SPE-driven changes. The top panel of Figure 3 shows the normal diurnal variation in electron number density, the second panel shows HO_x number density ($H + OH + HO_2$), the third panel NO_x number density ($N + NO + NO_2$), and the lower panel shows O_x ($O + O_3$). We use HO_x, NO_x and O_x rather than NO and O_3 as there are substantial diurnal variations in both the latter populations, which would lead to distracting features in the relative change plots presented below. In all cases these panels have units of $\log_{10}[\mathrm{cm}^{-3}]$.

The diurnal variation in the constituents is most clearly seen in the electron density and HO_x panels of Figure 3, but is much weaker for the NO_x and O_x panels. This is because the chemical lifetimes for the NO_x and O_x species are relatively long, while the rapid changes taking place during the diurnal cycle occur inside the family of species (i.e. NO_2 and NO). There is a gradual change present in the southern hemisphere HO_x and NO_x panels, due to increasing levels of sunlight caused by the seasonal lengthening of the periods with daytime conditions as seen in the electron density panels.

3.2 Proton Forcing

Ionization rates are calculated for the three possible representations of the Carrington SPE as described in *Verronen et al.* [2005], and are shown in Figure 4 with units of $\log_{10}[\mathrm{cm}^{-3}\mathrm{s}^{-1}]$. As the March 1991 spectrum leads to more high energy protons (>300 MeV) present in the SPE than the August 1972 spectrum, the ionization rates are more significant at lower altitudes (~20 km). However, the Weibull-fitted SPE spectrum for March 1991 also leads to additional lower energy protons (<20 MeV) relative to August 1972, causing the ionization rates to be larger than the August 1972 case for altitudes >~65 km. The hard spectra case (October 1989) has significant ionization rates present for the lowest altitudes considered in our modeling (at ~20 km), where the rates are several orders of magnitude higher than for either of the other spectra. In all cases the first ionization pulse is similar to the peak ionization rates seen for other large SPE events [e.g., *Verronen et al.*, Fig. 1, 2005, *Seppälä et al.*, Fig. 1, 2006], while the second pulse on 2 September 1859 is about one order of magnitude larger.

4. Modeling results

The ionization rates shown in Figure 4 are used to drive the SIC model. Hence we examine the altitude and time variation in the electron number density and the neutral atmospheric species (e.g., NO_x ($N + NO + NO_2$), HO_x ($H + OH + HO_2$), and O_x ($O + O_3$)), during the Carrington SPEs. The atmospheric changes modeled in our study mostly occur in the mesosphere and upper stratosphere, as determined by energy spectra of the precipitating protons. In the mesosphere changes in O_3 (or O_x) are primarily caused by increases in HO_x, although NO_x does play some role near 50 km and is important in O_x chemistry in the upper stratosphere. Ionization-produced NO_x and HO_x leads to the O_x changes as shown in the following figures.

4.1 Electron density variation

Figure 5 presents the Carrington SPE electron number density changes caused by the three selected SPE-spectra, relative to the control runs shown in Figure 3, shown for the northern hemisphere (left) and southern hemisphere (right) cases. The figure shows the ratio to represent the very large changes which occur. The electron density plots show very large increases during the period of direct SPE-forcing (i.e., 27 August-8 September 1859), with the two pulse time-structure of the SPE clearly seen in the electron density relative changes. The peak electron density changes in the 2nd pulse are roughly one order of magnitude larger than for the 1st pulse, as expected from the differences in the SPE forcing. The largest enhancements occur in the southern hemisphere, which is dominated by night-time ionospheric conditions. The three SPE spectra lead to rather similar electron density increases, of about 10^3-10^4 times in the 40-100 km altitude range. The primary difference between the 3 spectra considered is between the August 1972 and October 1989 cases below 40 km altitude, to the relative hardness of the spectra. Once the SPE forcing ends, the electron density rapidly returns to normal levels at most altitudes. The exception to this is a long-lived factor of 3-9 increase which occurs at ~80 km altitude, caused by the Lyman-α ionization of increased NO_x present after the SPE. Note that this electron density enhancement feature does not completely disappear, and is still present 10 days after the end of the SPE forcing. However, we are unable to determine the true recovery time of this enhancement, as it lasts beyond the timescale over which our model runs can be considered realistic. The length of the SIC-run needs to be limited due to the increasing significance of horizontal transport, in addition to vertical transport from adiabatic heating, neither of which are included in the 1D SIC model. In reality, the relatively small electron density enhancement feature is likely to dissipate more rapidly than shown here, due to transport mixing out the long-lived NO_x increase.

4.2 HO_x variation

Figure 6 presents the variation of HO_x, in the same format as Figure 5. Increases in HO_x are only significant around the times of the SPE-forcing, as the lifetime of HO_x is very short, and the majority of the SPE-produced HO_x rapidly decreases once forcing ends. As in the electron case, the increases appear more significant in the southern hemisphere as the background level of HO_x is larger in the daytime than the night (Figure 3). All three spectra lead to peak HO_x increases of about one order of magnitude from ~20-85 km, with the two "hard" SPE spectra causing significant HO_x increases to the lowest altitudes considered. Order-of-magnitude HO_x increases have been seen also during smaller, more recent SPE, one example being the January 2005 event [*Verronen et al.*, 2006; *Seppälä et al.*, 2006]. However these high enhancements have typically been restricted to mesospheric altitudes between 50-80 km. After the forcing, all the SPE spectra produce a long-lived HO_x increase of ~40% located around 60-80 km altitudes, present during the nighttime periods. This persistent HO_x increase is related to the increase of NO. Larger amounts of NO lead to increased ionization in the D-region, even at night-time because of Lyman-α radiation scattered from the geocorona being an important source of ions. Increased ionization leads to more HO_x production through ion chemistry during both day and night. However, this occurs on a relatively low level so that this change is only seen at night when the background production of HO_x, which is dependent upon solar radiation, is low. The persistent HO_x increase will influence O_x destruction at these altitudes, leading to a long-lived loss.

4.3 NO_x variation

The SPE-produced NO_x increases are shown in Figure 7, again in the same format as Figure 5. In this case, the NO_x increases are more significant in the northern hemisphere as the background levels of NO_x are significantly lower in the sunlight hemisphere (12 times less NO_x in the northern hemisphere), and hence the relative NO_x increase in the northern hemisphere is ~5 times larger than the southern hemisphere. The production rate is the same in both hemispheres, and while the loss rate is larger in the more sunlit northern hemisphere, the relative peak increases are also larger. The faster decay rates in the northern hemisphere due to additional levels of sunlight can be seen in this figure, such that the NO_x increases at the end of the SIC modeling period are larger in the southern hemisphere, even though the peak change is larger in the northern. The most significant NO_x increases occur from 40-85 km altitude, where the background NO_x levels are very low (Figure 3, panel 3). The SPE-produced increases are roughly 100-1000 times the background levels, and thus are much like creating lower thermospheric NO_x concentrations at mesospheric altitudes where NO_x concentrations are normally very low. Again, there is very little difference between the NO_x changes produced by the March 1991 and October 1989 SPE spectra, while the softer August 1972 spectra leads to 11-14 times less NO_x around 80 km altitude than for the harder spectra (depending on the hemisphere considered). The NO_x produced at altitudes below ~60 km altitudes is very long lived in all conditions as NO_x is normally destroyed by solar radiation, which has been largely absorbed at higher altitudes causing very little photodissociation of low-altitude enhancements. Once again, this is an area in which transport needs to be considered, and would be a reasonable topic for a future study.

4.4 O_x variation

The effect of the HO_x and NO_x increases on O_x is shown in Figure 8. In this case the relative changes (the ratio between the SPE run and the control run) are shown on a linear scale. During the peak SPE-forcing periods, O_x concentrations drop by 80-90% across an altitude range of 50-80 km, with minimum values of 11-13% of the ambient O_x. The two hard spectra representations produce unusually broad O_x decreases stretching over a wider altitude range than seen for most large SPE. For example, the large SPEs which occurred in January 2005 produced O_x decreases of about 80% over 70-80 km altitude [Fig2.,*Seppälä et al.*, 2004], while the Carrington SPE is likely to have led to a ~90% decrease over the wider altitude range of ~60-80 km. These very large decreases in O_x which occur during the SPE-forcing are caused by HO_x. However, this quickly returns to near normal levels at most altitudes (Figure 6) once the proton forcing has finished, after which the mesospheric O_x largely recovers. A long-lived but relatively small nighttime O_x decrease of 5%, at 60-80 km altitude remains after the forcing, caused by the previously identified HO_x feature in Figure 6. However, after the SPE forcing there is a significant long lived O_x decrease (O_x levels drop of ~40% when compared with normal levels) at ~45 km altitude, i.e. in the upper stratosphere. This is an unusually large decrease for a direct SPE effect upon these relatively low altitudes and is produced by the long-lived NO_x with an order of magnitude increase occurring at ~45 km altitude (Figure 7). The first pulse in the SPE leads directly to a ~10-20% O_x decrease at these altitudes, which is more typical for very large SPE [e.g. *Seppälä et al.*, 2004]. All the three possible Carrington spectra create this large low-altitude O_x decrease. Since protons of energy 30 MeV penetrate to ~50 km and the three proton flux spectra are normalized to the same value for proton energies >30 MeV, this was not unexpected. This is an indication of the extreme changes possible for the largest SPE, and is a feature not seen in "normal" large SPE, even those with unusually hard spectra [*Seppälä et al.*, 2004, 2008], where the relative SPE-produced NO_x increase are insignificant due to the very large background NO_x concentrations at these altitudes (Figure 3).

4.5 Synthesis

The three possible proton spectra representing the Carrington event lead to rather different atmospheric ionization rates (Figure 4), which in turn produce somewhat different responses for the electron number density profiles and neutral atmospheric constituents. There is also some difference in the relative response between the northern and southern hemisphere due to the relative levels of sunlight, either by pre-conditioning the background conditions (e.g., electrons, HO_x, NO_x), or by driving the direct loss rates (e.g., NO_x). In all cases the largest changes occur during the two-pulse solar proton event itself, across the ~12 days in which there is direct SPE forcing. During the period of direct SPE forcing the nature of the change depends somewhat upon the SPE-spectra and hemisphere considered. The first pulse of the SPE leads to changes which are similar to those produced by the largest SPE previously considered, while the second pulse generally drives considerably larger changes. After the period of SPE-forcing has finished there is much less difference in the calculated chemical effects between the different SPE-spectra and hemisphere calculations than the period during the SPE forcing. This is particularly the case for odd oxygen (O_x), likely the most important long-lived change driven by large SPE. In all cases considered here the Carrington SPE produces a significant and unusually strong long-lived O_x decrease (O_x levels drop by ~40%) at ~45 km altitude, i.e. in the upper stratosphere due to NO_x increases. As the nature of this NO_x increase does not vary significantly by SPE-spectra or hemisphere, there is relatively little variation in the long lived O_x decrease.

Thomas et al. [2007] used ionization rates scaled from the October 1989 SPE to describe the impact of the Carrington SPE upon long-lived ozone levels using a two dimensional atmospheric model. Figure 9 shows the variation in the O_3 column above 30 km altitude determined from our calculations, for the three possible Carrington spectra and considering both hemispheres. The maximum decrease in the >30 km O_3 column is ~9% for both hemispheres, with the somewhat softer spectra (March 1991) leading to maximum decrease of ~7%. As there is no immediate impact of the Carrington SPE upon O_3 below 30 km altitude, this 7-9% variation represents all the change in total column O_3 which would be produced by the SPE on short-time scales, before transport processes become significant. Transport processes are likely to cause a decent in altitude of the SPE-produced NO_x inside the winter pole, leading to larger decreases in O_x and to more significant decreases in column O_3. As the one dimensional SIC model does not extend to low altitudes, and does include some significant sources of vertical and horizontal transport, it is not possible to make a direct comparison with the results of *Thomas et al.* [2007] from their two dimensional model. However, the small differences between the calculated >30 km O_3 column indicates the atmospheric response of the Carrington SPE is not strongly dependent upon the spectra, suggesting that the calculations of *Thomas et al.* [2007] are likely to be reasonable, at least within the overall uncertainties associated with modeling this event.

The primary differences between the southern and northern hemispheric runs are due to the very differing levels of sunlight. In order to further test this, and to consider the possible "extreme" effect of the Carrington SPE, we have also undertaken a SIC-modeling run at the southern hemisphere location (70ºS, 0ºE) starting from 15 July, and thus considering a period in which there is almost no direct solar illumination. While it is complex to directly compare the results of this run with the earlier calculations described above due to the very different background conditions, there are no dramatic differences between the southern hemisphere polar winter run starting 15 July and the run for the actual Carrington event times. The minor differences (not shown) are dependent upon the levels of sunlight, as expected. For example, the NO_x loss at ~80 km is very low, such that almost all of the NO_x produced by the SPE remains to the end of the modeling run. In addition, the effect of the SPE during the forcing period is more significant, with deeper longer-lived O_x losses from 60-80 km altitude that recover more slowly (lasting 3-4 days more). However, the long-lived O_x decrease at 40-50 km altitude is slightly less significant in the polar night run (decreases of ~40% rather than ~60%). This is because the catalytic cycles of NO_x require atomic oxygen to be present, which is only released by photodissociation. While there are numerous minor differences between the polar night runs and the existing southern hemisphere runs, they are small enough that we can conclude the existing northern and southern hemisphere calculations provide a sufficiently accurate indication of the significance of the Carrington-event of 1859. Additional interhemispheric differences will also arise due to differences between the circulation patterns in both hemispheres and their seasonal variability, which is not captured in the existing 1D model used in our study. While this is likely to be significant when considering the long-time scale response, it is unlikely to produce large changes in the calculations as presented. Over time the relative importance of horizontal and vertical transport will increase, processes which are not fully included in the one dimensional SIC model. However, the SIC modeling does allow comparison between the immediate effects of the three different Carrington spectra in either hemisphere. As such, these calculations should also provide a reasonable estimate of the immediate impact of a future Carrington-like event striking the Earth's atmosphere.

5. Effect on HF communication

The additional ionospheric ionization caused by solar proton events lead to "polar blackouts", also known as "polar cap absorption (PCA)" events, which are disruptions to HF/VHF communications in high-latitude regions caused by attenuation in the ionospheric D-region [*Davies*, 1990]. The additional attenuation can make HF communications impossible throughout the polar regions, areas where HF communication is particularly important for the international aviation industry; on some occasions major airlines have cancelled trans-polar flights due to such space weather events [*Jones et al.*, 2005], while the practice of changing the flightpaths to avoid the poles leads to increased fuel consumption.

In order to characterize the ionospheric significance of the Carrington-SPE on HF attenuation levels, we consider the variation with time of the Highest Affected Frequency (HAF) during the SPE. The HAF is defined as the frequency which suffers a loss of 1 dB during vertical propagation from the ground, through the ionosphere, and back to ground. Radio frequencies lower than the HAF suffer an even greater loss. Here we determine the HAF by contrasting the SPE-produced electron density changes with those expected from Solar Flares, following the approach outlined in *Rodger et al.* [2006b]. As an example, an X20 flare, which has peak 0.1-0.8 nm X-ray fluxes of 2.0 mW m^{-2}, produces a HAF of 38 MHz. Flares of this magnitude lead to "extreme" Radio Blackouts, with essentially no HF radio contact with mariners or en-route aviators. NOAA has defined a Space Weather Scale for Radio Blackouts [*Poppe*, 2000], ranging from R1 describing a minor disruption due to an M1 flare (10 μW m^{-2} peak 0.1-0.8 nm X-ray flux) to R5 for the extreme blackout case described above. We will employ this scale to provide an indication of the severity of the SPE-induced polar blackouts.

Figure 10 shows the HF blackout estimates for the Carrington SPE. The left panels shows the blackouts estimated for the August 1972 spectra, while the right panels are for the March 1991 spectra, where the northern hemisphere results are in black and the southern hemisphere results in red. The HF blackouts estimated for October 1989 are very similar to the March 1991 case, due to the very similar electron density profiles (Figure 5), and hence are not shown in Figure 10.

The upper panels of Figure 10 show the equivalent peak X-ray flux in the 0.1-0.8 nm wavelength range which would cause the same ionosphere electron density change during a solar flare, represented using the H' parameter of *Wait and Spies* [1964]. For both the northern hemisphere and southern hemisphere cases, and both spectra, the SPE-produced disruptions are equivalent to very large equivalent peak X-ray fluxes. For context, there are about 175 solar flares with peak X-ray fluxes of X1 or above per solar cycle (~16 per year), and 8 flares >X10 per cycle. The upper panel of Figure 10 also indicates the X45 threshold, representing the largest solar flare peak X-ray flux measured since about 1976 [*Thomson et al.*, 2004; 2005]. In both cases the SPE-produced ionospheric disturbance peaks around the X45 threshold, and is larger than the X10 threshold for ~15.5 hours. In contrast, the X45 flare of 4 November 2003 led to X-ray fluxes which were >X10 for ~20 min [*Thomson et al.*, Fig. 2, 2004].

The lowest panels of Figure 10 presents the Highest Affected Frequency calculated from the equivalent peak X-ray powers following the empirically derived relationship between HAF and solar 0.1-0.8 nm X-ray flux provided by the *Space Environmental Forecaster Operations Manual* (1997). The NOAA Radio Blackout Scale has been added for comparison. While the peak HAF is smaller for the softer August 1972 spectra, in both cases and hemispheres the Carrington SPE would have produced polar blackouts equivalent to the "Extreme" threshold of the NOAA Radio Blackout Scale for a time period of ~15 hours, and led to some disturbances in polar HF communications for ~11-12 days. While this is long in comparison to most SPE disruptions, it is not wildly larger than the few days of disruption caused by most large SPE-events. As such, the polar communications disruptions associated with the Carrington SPE would not be severe, despite the exceptional nature of the SPE itself.

6. Discussion and Summary

The Carrington event of August/September 1859 was the most significant solar proton event (SPE) of the last 450 years, with about four times larger solar proton fluence than the largest event from the "spacecraft era" (August 1972). The space weather event which occurred at this time produced the most intense geomagnetic storm in recorded history and the first visual observation of a white-light solar flare. Recently, much attention has focused upon increasing our understanding of the Carrington event, in order to better quantify the impact of extreme space weather events. In this study we have used new findings as to the nature of the Carrington event, adopting an intensity-time profile for the >30 MeV solar proton flux, and examining the relative atmospheric response to three different SPE-energy spectra which have previously been used to represent the Carrington SPE. Cosmogenic isotope concentrations have indicated that the Carrington SPE likely had a comparatively soft energy spectrum, for example similar to those measured for the August 1972 or March 1991 SPE, rather than the October 1989 SPE spectra sometimes used to model the impact of the Carrington SPE. The Sodankylä Ion and Neutral Chemistry (SIC) model has been used to estimate the impact of the Carrington event to the neutral atmosphere and the ionosphere, and the disruption to HF communication.

As seen in the SIC-output plots described in this paper, large changes in electron density and atmospheric constituents occur during the period of SPE-forcing, which depend upon the nature of the spectrum and also on the hemisphere considered. This is particularly significant for the electron density increases. However, the most important SPE-driven atmospheric response is the long-lived O_x decreases in the upper stratosphere (O_x levels drop by ~40% of the normal level). This change does not significantly vary between the 3 spectra, or between the 2 hemispheres, due to the very small differences in the long-lived low-altitude NO_x increases which produce the O_x decreases. All the three possible Carrington spectra create this large low-altitude O_x decrease due to the very large >30 MeV proton fluxes present in the normalized spectra. This is an indication of the extreme changes possible for the very largest SPE, and is not a feature seen previously for "normal" large SPE, even those with unusually hard spectra.

We have also characterized the ionospheric significance of the Carrington-SPE on HF attenuation levels. Should a Carrington-level event occur in the current era, it would cause disruptions to HF/VHF communications in high-latitude regions, making HF communications impossible throughout the polar regions for some time. This could have a significant impact on the routing of trans-polar aeroplane travel. The Carrington SPE would have produced polar blackout equivalent to the "Extreme" threshold of the NOAA Radio Blackout Scale for a time period of ~15 hours, and led to some disturbances in polar HF communications over a time period of ~11-12 days, (i.e., during the period of direct SPE forcing). While this is long in comparison to most SPE disruptions, it is not wildly larger than the few days of disruption caused by most large SPE-events. As such, the polar communications disruptions associated with the Carrington SPE would not be particularly severe, despite the exceptional nature of the SPE itself.

In general, the atmospheric and ionospheric response is somewhat different between the August 1972 or March 1991 SPE spectra, while the calculations using the March 1991 and October 1989 SPE spectra are very similar to one another. Thus while cosmogenic isotope concentrations from ice-cores indicate that the Carrington-SPE was comparatively soft, the conclusions of previous modeling studies into the atmospheric response of the Carrington SPE which have used rather hard spectra, and specifically the October 1989 SPE spectra, are likely to be reasonable, at least within the overall uncertainties associated with modeling this event. This is particularly important to the conclusions of *Thomas et al.* [2007], who used ionization rates scaled from the October 1989 SPE to describe the impact of the Carrington SPE upon long-lived ozone levels. These authors concluded that the globally averaged column-ozone would decrease by as much as 4%, recovering slowly over several years. While this ozone depletion is small in a global sense, it is accompanied by much larger decreases in the poles, with long-lived polar ozone losses which are similar to those calculated in our study. As noted by *Thomas et al.*, even small increases in UVB can be harmful to many life forms. In addition, changes in the chemical balance of the upper and middle stratosphere may be associated with changes in polar winds and temperatures, and may even lead to few degree variations in sea-level temperatures [*Rozanov et al.*, 2005].

Acknowledgments. CJR would like to thank Gillian Rodger of Manchester for her support. PTV and AS are partly funded by the Academy of Finland through project 123275, Thermosphere and Mesosphere affecting the Stratosphere. AS would also like to thank the Academy of Finland for their support of her work through the EPPIC project.

References

Banks, P. M., and G. Kockarts (1973), Aeronomy, vol. B, chap. 15, Academic Press.

Beer, J., A. Blinov, G. Bonani, R. C. Finkel, H. J. Hofmann, B. Lehmann, H. Oeschger, A. Sigg, J. Schwander, T. Staffelbach, B. Stauffer, M. Suter, and W. Wötfli (1990), Use of ^{10}Be in polar ice to trace the 11-year cycle of solar activity, Nature, 347, 164–166, doi:10.1038/347164a0.

Boteler, D. H. (2006), The super storms of August/September 1859 and their effects on the telegraph system, Advances Space Res., 38(2), 159-172.

Brasseur, G., and S. Solomon (1986), Aeronomy of the Middle Atmosphere, second ed., D. Reidel Publishing Company, Dordrecht.

Carrington, R.C. (1860), Description of a singular appearance seen in the Sun on September 1, 1859. Monthly Not. R. Astron. Soc. 20, 13–15.

Clilverd, M. A., A. Seppälä, C. J. Rodger, N. R. Thomson, P. T. Verronen, E. Turunen, Th. Ulich, J. Lichtenberger, and P. Steinbach, Modeling polar ionospheric effects during the October-November 2003 solar proton events, *Radio Sci.*, 41(2), doi: 10.1029/2005RS003290, 2006.

Chabrillat, S., G. Kockarts, D. Fonteyn, and G. Brasseur (2002), Impact of molecular diffusion on the CO_2 distribution and the temperature in the mesosphere, Geophys. Res. Lett., 29, 1-4.

Crutzen, P. J., I. S. A. Isaksen, and G. C. Reid (1975), Solar proton events: Stratospheric sources of nitric oxide, Science, 189, 457–458.

Crutzen, P., and S. Solomon (1980), Response of mesospheric ozone to particle precipitation, Planetary and Space Science, 28, 1147–1153.

Davies, K. (1990), Ionospheric radio, Peter Peregrinus, London.

Hedin, A. E. (1991), Extension of the MSIS Thermospheric model into the middle and lower Atmosphere, J. Geophys. Res., 96, 1159-1172.

Jackman, C. H., and R. D. McPeters (1985), The responce of ozone to solar proton events during solar cycle 21: A theoretical interpretation, J. Geophys. Res., 90, 7955–7966.

Jackman, C. H., and P. E. Meade (1988), Effect of solar proton events in 1978 and 1979 on the odd nitrogen abundance in the middle atmosphere, J. Geophys. Res., 93, 7084–7090.

Jackman, C. H., A. R. Douglass, R. B. Rood, R. D. McPeters, and P. E. Meade (1990), Effect of solar proton events on the middle atmosphere during the past two solar cycles as computed using a two-dimensional model, J. Geophys. Res., 95, 7417–7428.

Jackman, C. H., J. E. Nielsen, D. J. Allen, M. C. Cerniglia, R. D. McPeters, A. R. Douglass, and R. B. Rood (1993), The effects of the October 1989 solar proton events on the stratosphere as computed using a three-dimensional model, Geophys. Res. Lett., 20, 459–462.

Jackman, C. H., M. C. Cerniglia, J. E. Nielsen, D. J. Allen, J. M. Zawodny, R. D. McPeters, A. R. Douglass, J. E. Rosenfield, and R. B. Hood (1995), Two-dimensional and three-dimensional model simulations, measurements, and interpretation of the October 1989 solar proton events on the middle atmosphere, J. Geophys. Res., 100, 11,641–11,660.

Jackman, C. H., Fleming, E. L., Chandra, S., Considine, D. B., and Rosenfield, J. E., Past, present, and future modeled ozone trends with comparisons to observed trends (1996), J. Geophys. Res., 101 , 28 753–28 768.

Jackman, C. H., E. L. Fleming, and F. M. Vitt (2000), Influence of extremely large solar proton events in a changing stratosphere, J. Geophys. Res., 105, 11,659–11,670.

Jackman, C. H., R. D. McPeters, G. J. Labow, E. L. Fleming, C. J. Praderas, and J. M. Russel (2001), Northern hemisphere atmospheric effects due to the July 2000 solar proton events, Geophys. Res. Lett., 28, 2883–2886.

Jackman, C. H., R. G. Roble, and E. L. Fleming (2007), Mesospheric dynamical changes induced by the solar proton events in October–November 2003, *Geophys. Res. Lett.*, *34*, L04812, doi:10.1029/2006GL028328.

Jones, J. B. L., R.D. Bentley, R. Hunter, R.H.A. Iles, G.C. Taylor and D.J. Thomas (2006), Space weather and commercial airlines, Advances Space Res., 36(12), 2258-2267.

MacNamara, L. F. (1985), High frequency radio propagation, in Handbook of Geophysics and the Space Environment, edited by A. S. Jursa, Chapter 10, pp. 45-65, Air Force Geophys. Lab., U. S. Air Force.

McCracken, K. G., G. A. M. Dreschhoff, E. J. Zeller, D. F. Smart, and M. A. Shea (2001a), Solar cosmic ray events for the period 1561–1994. 1. Identification in polar ice, 1561–1950. J. Geophys. Res. 106 (A10), 21585–21598.

McPeters, R. D., and C. H. Jackman (1985), The response of ozone to solar proton events during solar cycle 21: the observations, J. Geophys. Res., 90, 7945–7954.

Nevanlinna, H. (2006), A study on the great geomagnetic storm of 1859: Comparisons with other storms in the 19th century, Adv. in Space Res., 38 (2), 180-187.

Odenwald, S., J. Green, and W. Taylor (2006), Forecasting the impact of an 1859-calibre superstorm on satellite resources, Advances Space Res., 38(2), 280-297.

Poppe, B. (2000), New scales help public, technicians understand space weather, Eos Trans., Vol. 81 (29), 322, July 18.

Rodger, C. J., M. A. Clilverd, P. T. Verronen, Th. Ulich, M. J. Jarvis, and E. Turunen (2006a), Dynamic geomagnetic rigidity cutoff variations during a solar proton event, J. Geophys. Res., 111, A04222, doi:10.1029/2005JA011395.

Rodger, C. J., M. A. Clilverd, Th. Ulich, P. T. Verronen, E. Turunen, and N. R. Thomson (2006b), The atmospheric implications of Radiation Belt Remediation, Annales Geophys., 24(7), 2025 - 2041, SRef-ID: 1432-0576/ag/2006-24-2025.

Seppälä, A., P. T. Verronen, E. Kyrölä, S. Hassinen, L. Backman, A. Hauchecorne, J. L. Bertaux, and D. Fussen (2004), Solar proton events of October-November 2003: Ozone depletion in the Northern hemisphere polar winter as seen by GOMOS/Envisat, Geophys. Res. Lett., 31(19), L19,107, doi:10.1029/2004GL021042.

Seppälä, A., P. T. Verronen, V. F. Sofieva, J. Tamminen, E. Kyrölä, C. J. Rodger, and M. A. Clilverd (2006), Destruction of the tertiary ozone maximum during a solar proton event, Geophys. Res. Lett., 33, L07804, doi:10.1029/2005GL025571.

Seppälä, A., M. A. Clilverd, C. J. Rodger, P. T. Verronen, and E. Turunen (2008), The effects of hard spectra solar proton events on the middle atmosphere, J. Geophys. Res., in press.

Shea, M. A., D. F. Smart, K. G. McCracken, G. A. M. Dreschoff, and H. E. Spence (2006), Solar proton events for 450 years: The Carrington event in perspective, Adv. Space Res., 38 (2), 232-238.

Shea, M. A., and D. F. Smart (2006), Geomagnetic cutoff rigidities and geomagnetic coordinates appropriate for the Carrington flare epoch, Adv. Space Res. 38 (2006), pp. 209–214.

Shimazaki, T. (1984), Minor Constituents in the Middle Atmosphere (Developments in Earth and Planetary Physics, No 6), D. Reidel Publishing Co., Dordrecht, Netherlands.

Smart, D. F., M. A. Shea, and K. G. McCracken (2006), The Carrington event: Possible solar proton intensity–time profile, Adv. Space Res., 38 (2), 215-225.

Solomon, S., D. W. Rusch, J.-C. Gérard, G. C. Reid, and P. J. Crutzen (1981), The effect of particle precipitation events on the neutral and ion chemistry of the middle atmosphere: II. Odd hydrogen, Planet. Space Sci., 8, 885–893.

Solomon, S., G. C. Reid, D. W. Rusch, and R. J. Thomas (1983), Mesospheric ozone depletion during the solar proton event of July 13, 1982 Part II. Comparisons between theory and measurements, Geophys. Res. Lett., 10, 257–260.

Space Environmental Forecaster Operations Manual, page 4.3.1, 55th Space Weather Squadron, Falcon AFB, USAF, 21 October 1997. As referenced by the NOAA Space Environment Center at http://www.swpc.noaa.gov/dregion/dregionDoc.html

Rozanov, E., L. Callis, M. Schlesinger, F. Yang, N. Andronova, and V. Zubov (2005), Atmospheric response to NOy source due to energetic electron precipitation, Geophys. Res. Lett., 32, L14811, doi:10.1029/2005GL023041.

Thomas, B. C., C. H. Jackman, and A. L. Melott (2007), Modeling atmospheric effects of the September 1859 solar flare, Geophys. Res. Lett., 34, L06810, doi:10.1029/ 2006GL029174.

Thomas, L., and M. R. Bowman (1986), A study of pre-sunrise changes in negative ions and electrons in the D-region, Ann. Geophys., 4, 219-228.

Thomson, N. R., C. J. Rodger, and R. L. Dowden (2004), Ionosphere gives size of greatest solar flare, *Geophys. Res. Lett.*, 31(6), L06803, 10.1029/2003GL019345.

Thomson, N. R., C. J. Rodger, and M. A. Clilverd (2005), Large solar flares and their ionospheric D-region enhancements, *J. Geophys. Res.*, 110, A06306, doi:10.1029/2005JA011008.

Tobiska, W. K., T. Woods, F. Eparvier, R. Viereck, L. D. B. Floyd, G. Rottman, and O. R. White (2000), The SOLAR2000 empirical solar irradiance model and forecast tool, J. Atmos. Terr. Phys., 62, 1233-1250.

Townsend, L. W. (2003), Carrington flare of 1859 as a prototypical worst-case solar energetic particle event, IEEE Trans. Nucl. Sci., 50(6), 2307-2309.

Tsurutani, B. T., W. D. Gonzalez, G. S. Lakhina, and S. Alex (2003), The extreme magnetic storm of 1–2 September 1859, J. Geophys. Res., 108(A7), 1268, doi:10.1029/2002JA009504.

Turunen, E., H. Matveinen, J. Tolvanen, and H. Ranta (1996), D-region ion chemistry model, in STEP Handbook of Ionospheric Models, edited by R. W. Schunk, pp. 1-25, SCOSTEP Secretariat, Boulder, Colorado, USA.

Turunen, E., P. T. Verronen, A. Seppälä, C. J. Rodger, M. A. Clilverd, J. Tamminen, C. F. Enell and Th. Ulich (2008), Impact of different precipitation energies on NO_x generation during geomagnetic storms, J. Atmos Sol.-Terr. Phys., in press.

Verronen, P. T., E. Turunen, Th. Ulich, and E. Kyrölä (2002), Modelling the effects of the October 1989 solar proton event on mesospheric odd nitrogen using a detailed ion and neutral chemistry model, Ann. Geophys., 20, 1967-1976.

Verronen, P. T., A. Seppälä, M. A. Clilverd, C. J. Rodger, E. Kyrölä, C-F. Enell, Th. Ulich, E. and Turunen (2005), Diurnal variation of ozone depletion during the October-November 2003 solar proton event, J. Geophys. Res., 110(A9), doi:10.1029/2004JA010932.

Verronen, P. T., A. Seppälä, E. Kyrölä, J. Tamminen, H. M. Pickett, E. and Turunen, Production of odd hydrogen in the mesosphere during the january 2005 solar proton event (2006), Geophys. Res. Lett., 33, L24811, doi:10.1029/2006GL028115.

Wait, J. R., and K. P. Spies (1964), Characteristics of the Earth-ionosphere waveguide for VLF radio waves, NBS Tech. Note 300, Nat. Inst. of Stand. and Technol., Gaithersburg, Md..

Xapsos, M. A., J. L. Barth, E. G. Stassinopoulos, S. R. Messenger, R. J. Walters, G. P. Summers, and E. A. Burke (2000), Characterizing solar proton energy spectra for radiation effects applications, IEEE Trans. Nuclear Sci., 47(6).

M. A. Clilverd and A. Seppälä, Physical Sciences Division, British Antarctic Survey (NERC), High Cross, Madingley Road, Cambridge CB3 0ET, England, U.K. (e-mail: macl@bas.ac.uk, annika.seppala@fmi.fi).

C. J. Rodger, Department of Physics, University of Otago, P.O. Box 56, Dunedin, New Zealand. (email: crodger@physics.otago.ac.nz).

E. Turunen, Sodankylä Geophysical Observatory, University of Oulu, Sodankylä, Finland. (email: esa@sgo.fi).

P. T. Verronen, Earth Observation, Finnish Meteorological Institute, P.O. Box 503 (Erik Palménin aukio 1), FI-00101 Helsinki, Finland. (email: pekka.verronen@fmi.fi).

Table 1. Weibull fitting parameters used in equation 1 to represent the differential SPE fluxes of the Carrington event with the 4 different energy spectra as shown in Figure 1.

Date	Φ_0	k	α
4 August 1972	5.0033×10^{10}	0.0236	1.108
29 September 1989	4.5751×10^{11}	0.877	0.3841
19 October 1989	4.4280×10^{12}	2.115	0.2815
23 March 1991	1.4039×10^{12}	0.972	0.441

Figures

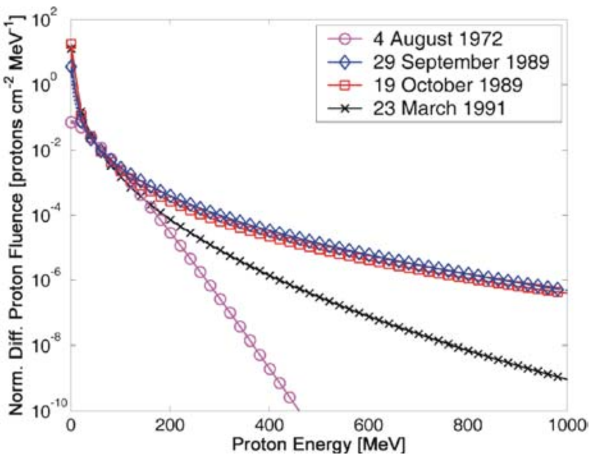

Figure 1. Comparison between the normalised differential fluences which have been used to describe the Carrington event, based on four previous SPE. The values shown have been normalised to the Carrington-level >30 MeV fluence of 1.9×10^{10} protons cm^{-2}. [See the online version for the color version of this figure].

Wednesday, September 17, 2008

666

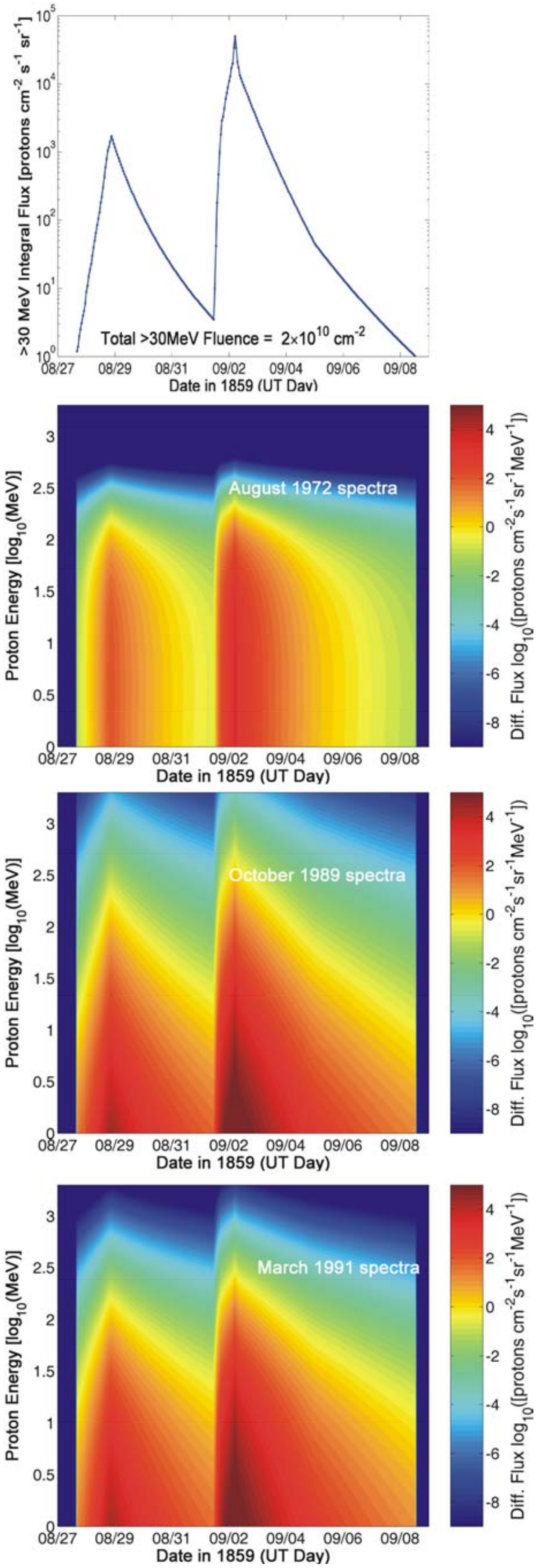
>30 MeV Integral Flux [protons cm-2 s-1 sr-1]
Total >30MeV Fluence = 2×10^10 cm^-2
Date in 1859 (UT Day)
08/27
08/29
08/31
09/02
09/04
09/06
09/08
Proton Energy [log10(MeV)]
August 1972 spectra
October 1989 spectra
March 1991 spectra
Diff. Flux log10([protons cm-2s-1sr-1MeV-1])

Figure 2. Proton fluxes used to describe the Carrington event SPE. The upper panel shows the >30 MeV intensity-time proton profile [after *Smart et al.*, Fig. 12, 2006]. The lower 3 panels present the different time-varying differential proton fluxes used in this study to describe Carrington-level SPE. [See the online version for the color version of this figure].

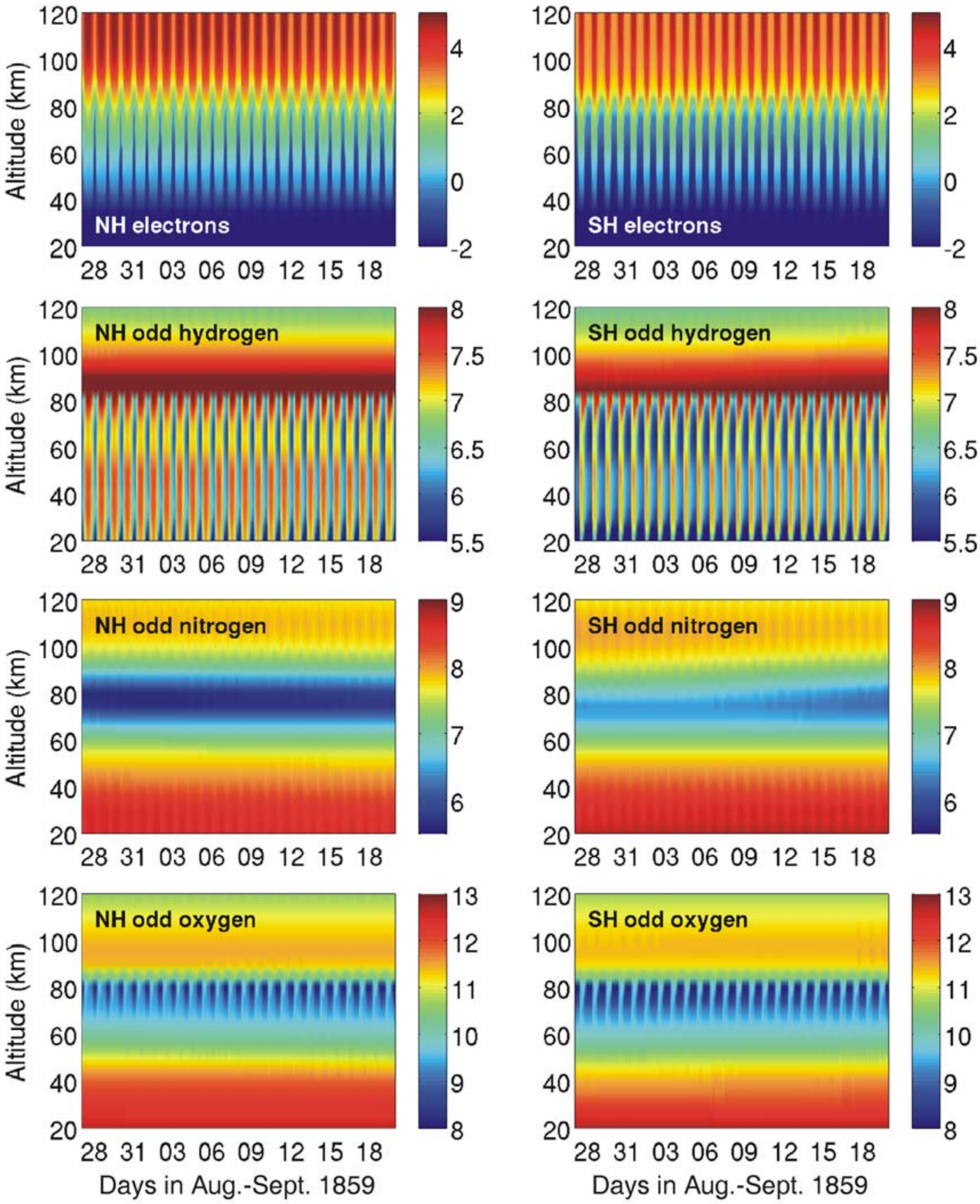

Figure 3. The results of a SIC modeling run without any SPE-forcing (i.e., zero precipitating proton fluxes), showing the calculated "normal" conditions for the northern (left) and southern (right) hemispheres. Units are shown in $\log_{10}[cm^{-3}]$. [See the online version for the color version of this figure].

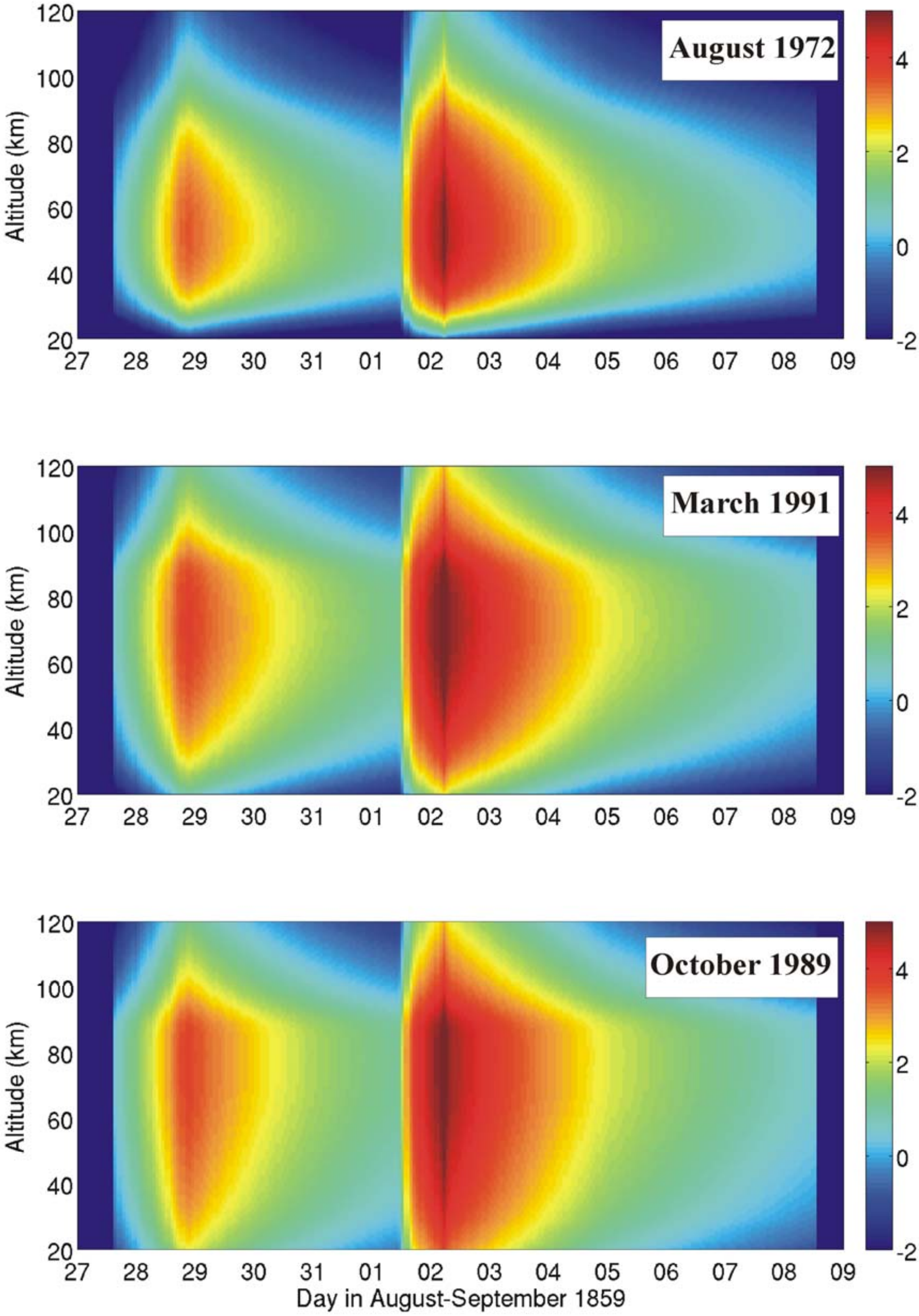
August 1972
March 1991
October 1989
Altitude (km)
120
100
80
60
40
20
27 28 29 30 31 01 02 03 04 05 06 07 08 09
4
2
0
-2
Day in August-September 1859

Figure 4. Atmospheric ionization rates calculated from the SPE fluxes shown in the lower 3 panels of Figure 2, given in units of $\log_{10}[cm^{-3}s^{-1}]$. [See the online version for the color version of this figure].

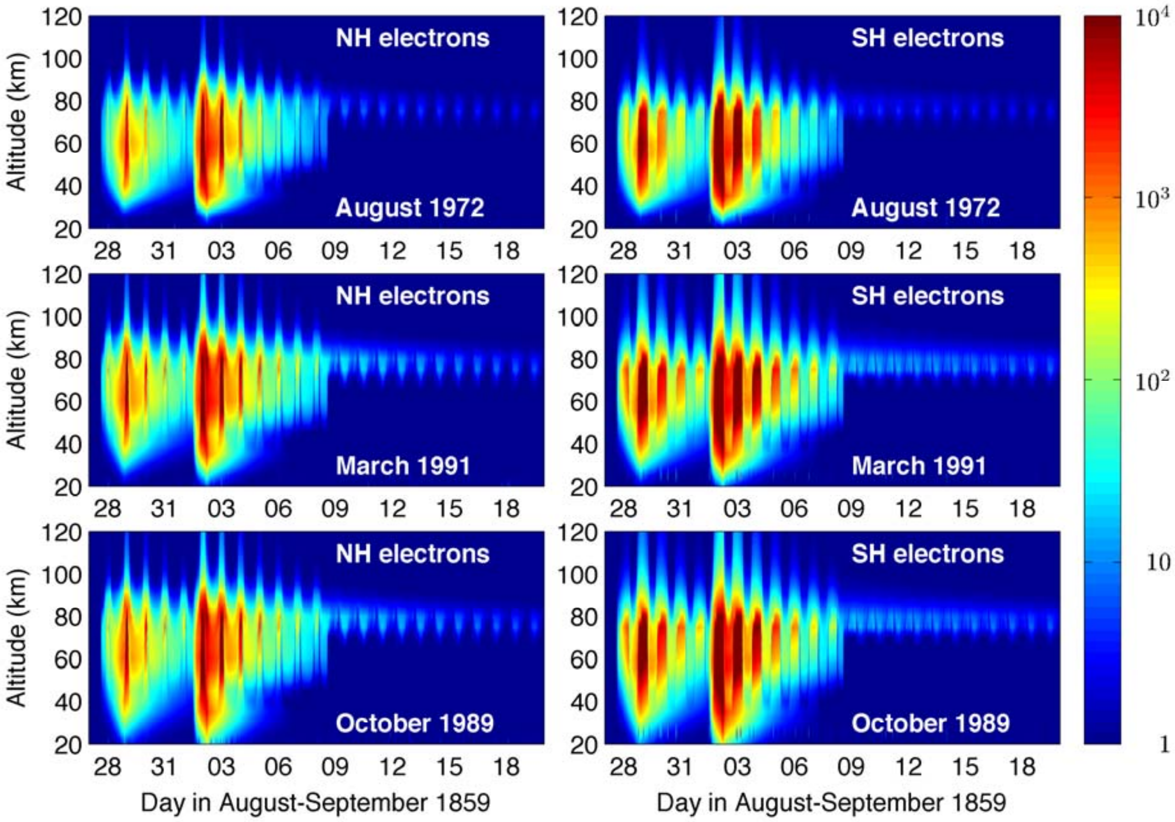

Figure 5. SPE-driven changes in electron number density determined from the SIC model for the varying SPE spectra, and show as the ratio to the control run (Figure 3). The left panels are for the northern hemisphere, while the right are the southern hemisphere. [See the online version for the color version of this figure].

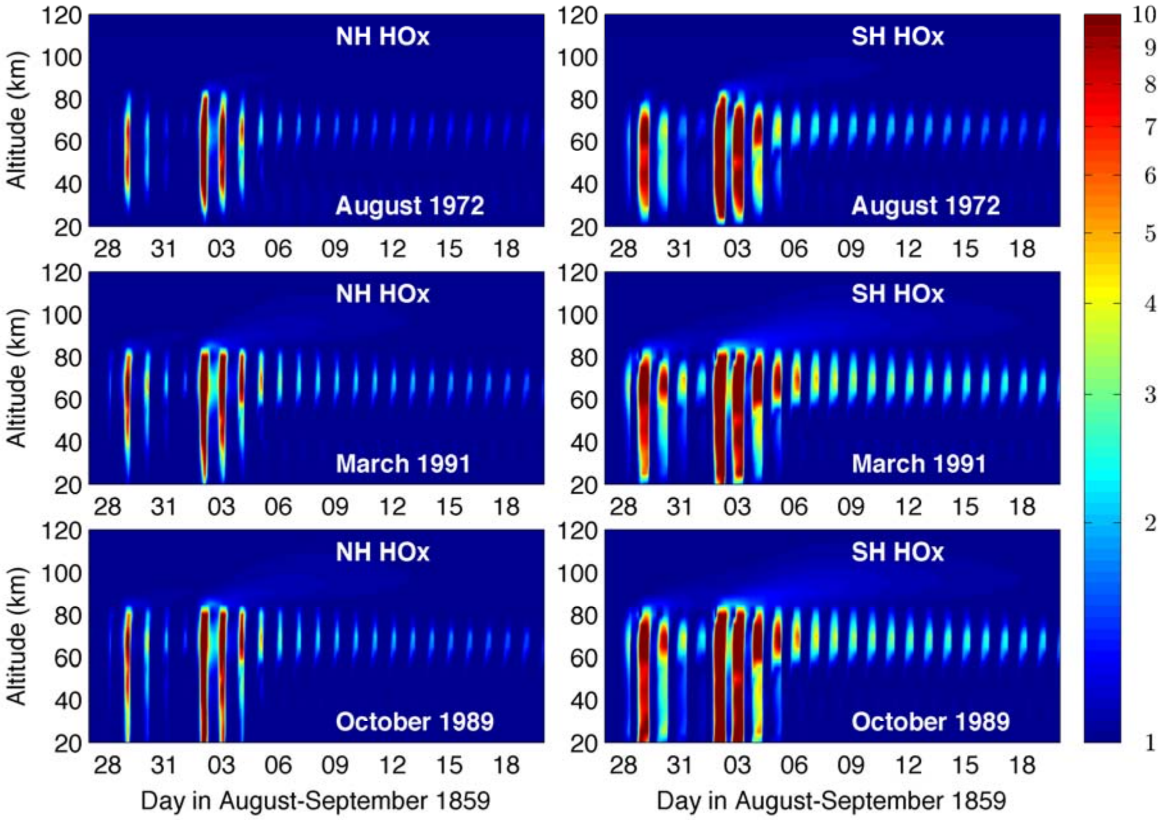

Figure 6. SPE-driven changes in odd hydrogen (HO_x) determined from the SIC model for the varying SPE spectra, and show as the ratio to the control run (Figure 3). The left panels are for the northern hemisphere, while the right are the southern hemisphere. [See the online version for the color version of this figure].

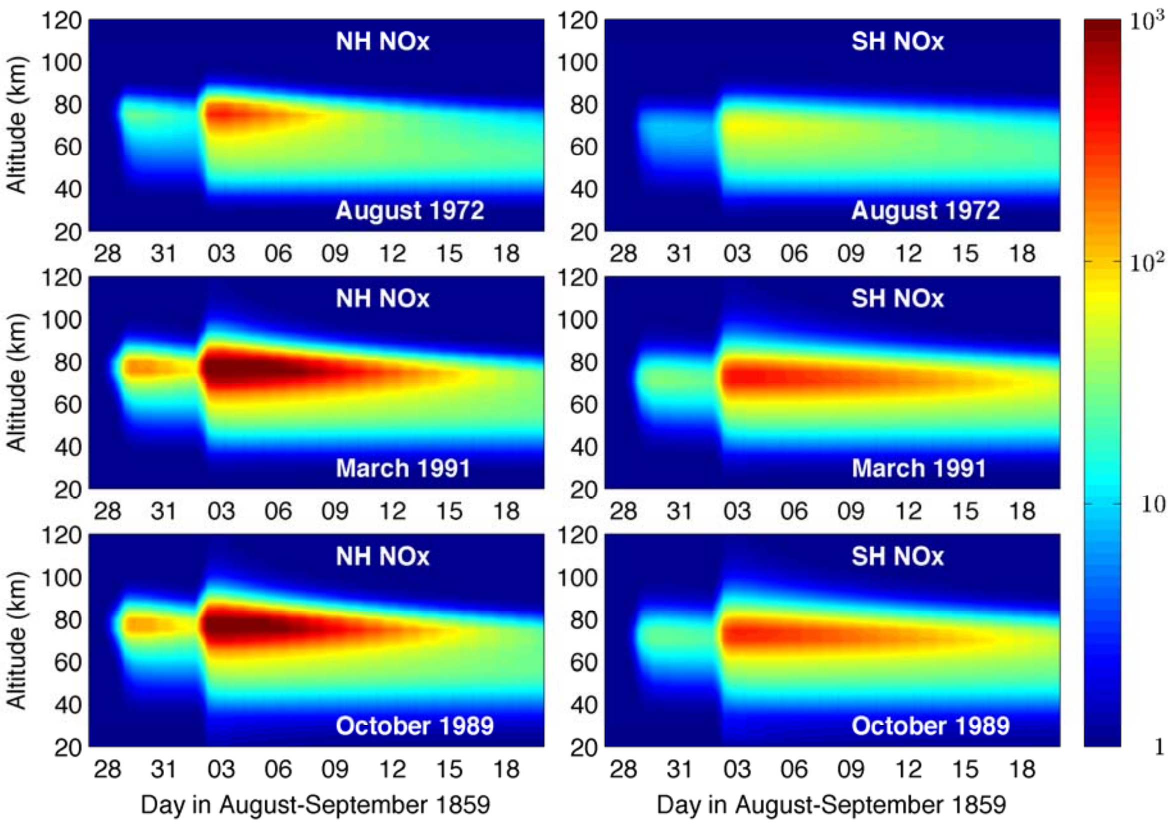

Figure 7. SPE-driven changes in odd nitrogen (NO_x) determined from the SIC model for the varying SPE spectra, and show as the ratio to the control run (Figure 3). The left panels are for the northern hemisphere, while the right are the southern hemisphere. [See the online version for the color version of this figure].

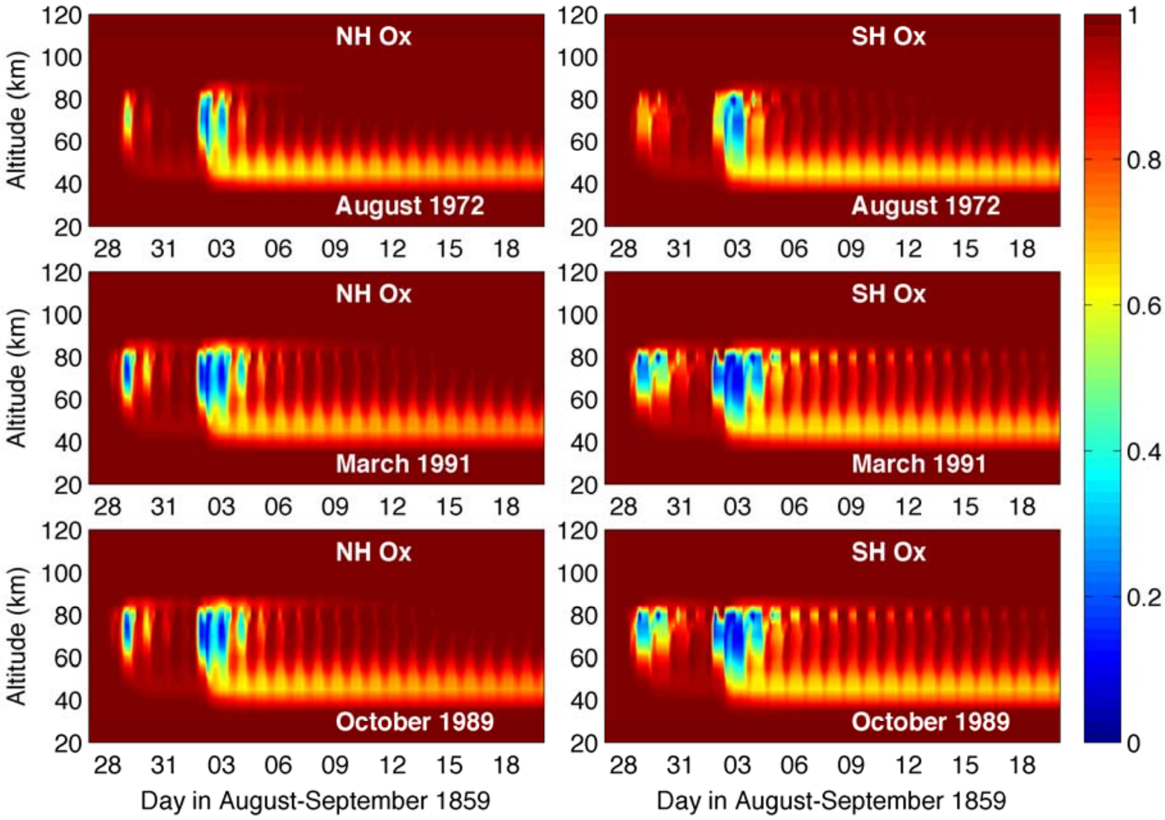

Figure 8. SPE-driven changes in odd oxygen (O_x) determined from the SIC model for the varying SPE spectra, and show as the linear ratio to the control run (Figure 3). The left panels are for the northern hemisphere, while the right are the southern hemisphere. [See the online version for the color version of this figure].

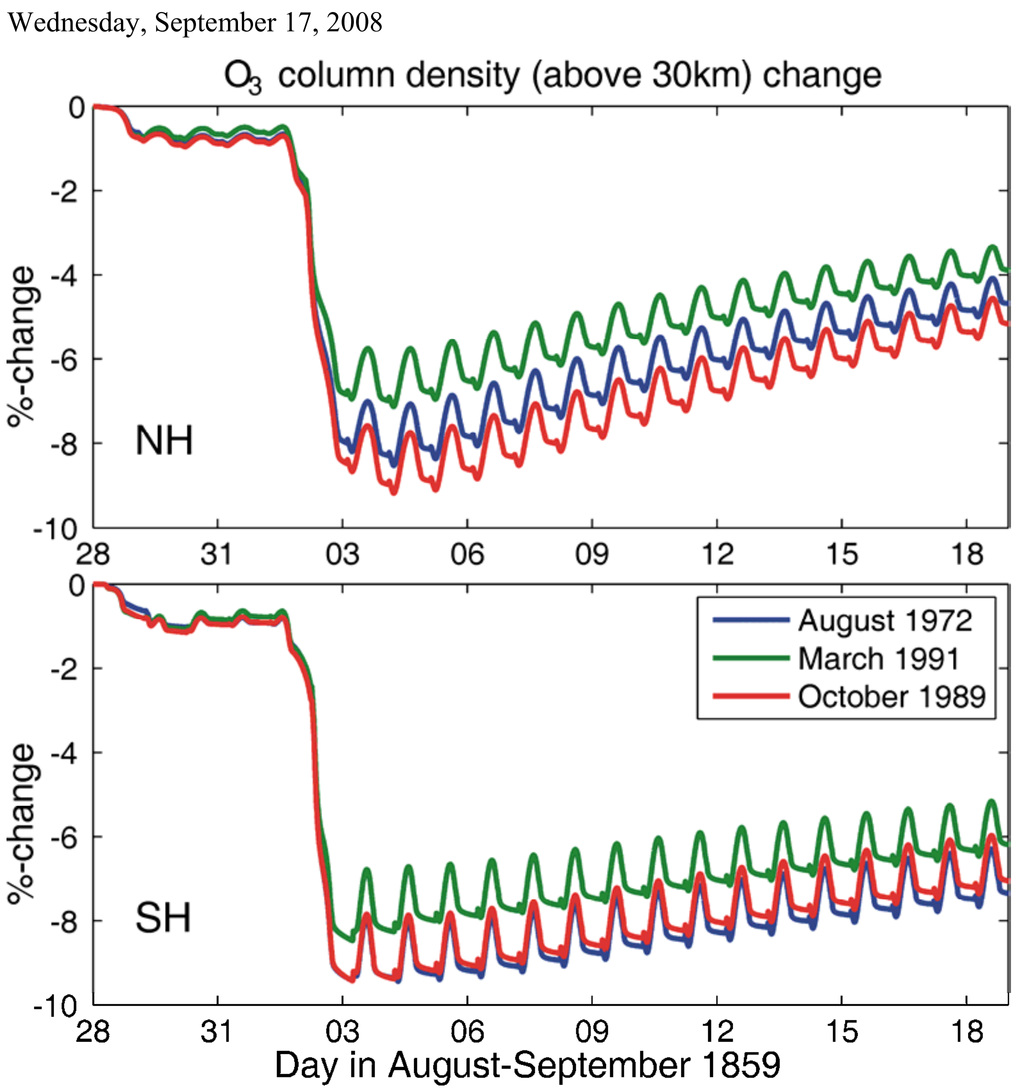

Figure 9. SPE-driven percentage changes in the >30 km altitude O_3 total column for varying Carrington SPE spectra. The upper panel shows the changes for the northern hemisphere (NH), while the lower is for the southern hemisphere (SH). [See the online version for the color version of this figure].

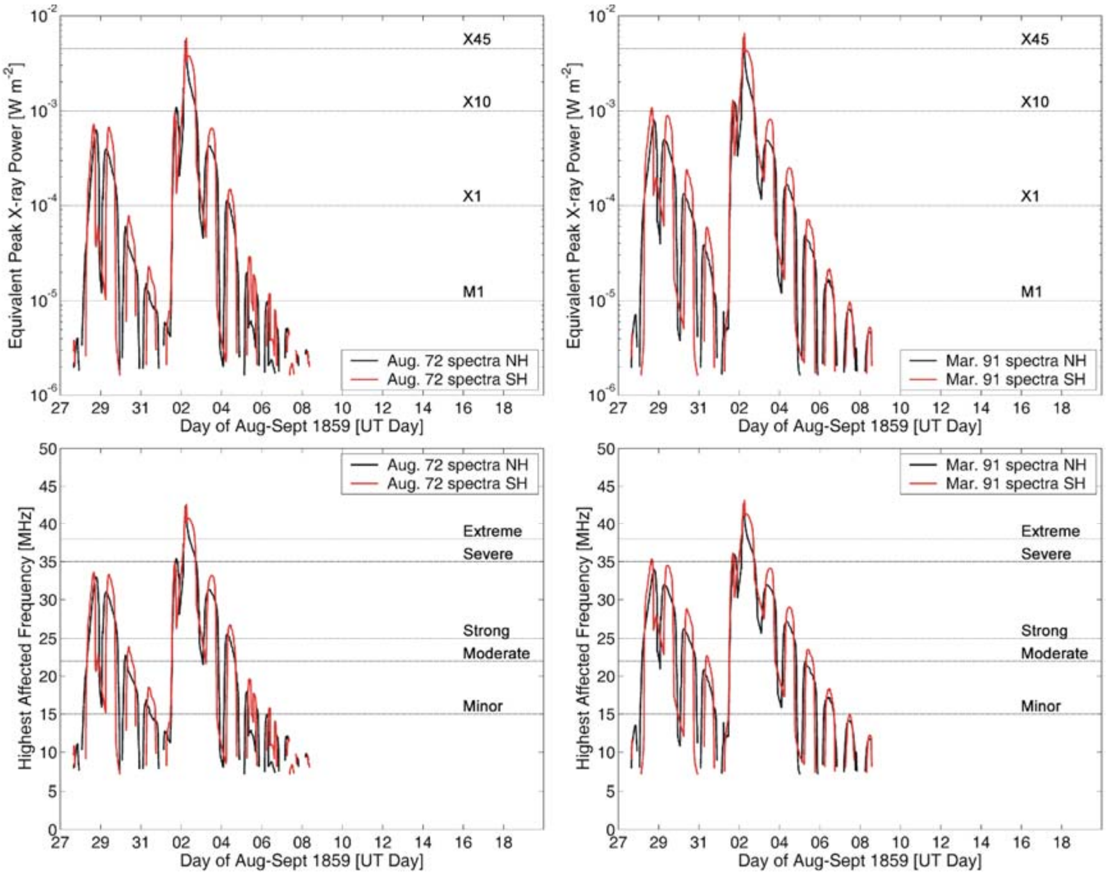

Figure 10. Estimate of the severity of the Carrington-SPE forced HF polar blackout for the August 1972 (left) and March 1991 (right) SPE-spectra. The upper panel shows the equivalent peak X-ray fluxes in the 0.1-0.8 nm range which would cause the same ionospheric change during a solar flare. The lower panel is the Highest Affected Frequency calculated from the equivalent peak X-ray flux. The NOAA Radio Blackout Scale has been added for comparison. [See the online version for the color version of this figure].